Surface-acoustic-wave-controlled optomechanically induced transparency in a hybrid piezo-optomechanical planar distributed Bragg-reflector-cavity system

Shi-Chao Wu [1,2,3] Li Zhang,[1,2] Jian Lu,[1] Li-Guo Qin,[1,4] and Zhong-Yang Wang[1,*]

[1]*Shanghai Advanced Research Institute, Chinese Academy of Sciences, Shanghai 201210, China*
[2]*University of Chinese Academy of Sciences, Beijing 100000, China*
[3]*Jiangsu Ocean University, School of Sciences, Lianyungang 320700, China*
[4]*Department of Physics, Shanghai University of Engineering Science, Shanghai 201620, China*

We propose a scheme that can generate tunable optomechanically induced transparency in a hybrid piezo-optomechanical cavity system. The system is composed of a high-quality planar distributed Bragg reflector cavity modified with an embedded Gaussian-shaped defect. Moreover, interdigitated transducers are fabricated on the surface of the cavity to generate surface acoustic waves. Under the actuation of the surface acoustic wave, the upper Bragg mirrors can be vibrated as a bulk acoustic resonator, and the distributed Bragg reflector cavity becomes a standard three-level optomechanical system. In this situation, we show that when a strong pump optical field and a weak probe optical field are simultaneously applied to the hybrid optomechanical cavity system, optomechanically induced transparency occurs under the quantum interference between different energy-level pathways. Our scheme can be applied in the fields of optical switches and quantum information processing in solid-state quantum systems.

I. INTRODUCTION

In the field of quantum information, many types of artificial atomic systems have been proposed to regulate and manipulate the processing of optical or microwave information, including superconducting quantum circuits [1,2], nitrogen-vacancy (N-V) centers [3,4], semiconductor quantum dots [5,6], and distributed Bragg reflector (DBR) cavities [7,8]. Furthermore, since most of these artificial atomic systems can be coupled with both photon and phonon modes, the optical information can also be operated by modulating the phonon modes. There are many methods to control the phonon modes; for example, phonon modes can be driven by the radiation pressure of the optical field or microwave field [9,10]. Moreover, in recent experiments, the phonon modes can be driven by different types of external mechanical fields, such as the Lorentz force and piezoelectric force [11,12]. A representative mechanical field is the surface acoustic wave (SAW) [13–20], which is generated by the piezoelectric effect. Since piezoelectric materials are widely used in optically DBR-cavity systems, the SAW can be applied to modulate the optical properties of DBR-cavity systems by controlling the phonon modes [14].

The SAW is a type of phononlike excitation containing mechanical vibration modes [13–18]. It is electrically generated on the surface of the piezoelectric substrate using interdigital transducers (IDTs), which are driven by the radio-frequency (RF) voltage source. Furthermore, the SAW contains both transverse and longitudinal vibration modes; when it propagates along the surface of the substrate, it simultaneously propagates downward. The velocity of the SAW propagating along the surface is determined by the material performance of the substrate. When the SAW propagates downward, its vibration frequency can be adjusted with the design of the IDTs, and the extension depth below the surface is approximately one wavelength of the SAW. Accordingly, the surface of the substrate in the vertical direction is vibrated as a bulk acoustic resonator (BAR), which can be considered a standard mechanical resonator [4]. Moreover, the intrinsic damping rate of the BAR is determined by the SAW mode, which is equal to the linewidth of the SAW mode. In the related research, the quality factor of the BAR can exhibit the order of 10^5. Correspondingly, its frequency can exceed the order of gigahertz, and its intrinsic damping rate can exceed the order of 10 kHz [19–21].

Planar DBR-cavity systems have been applied to realize light-sound interactions in related experiments [22]. Generally, the quality of the DBR cavities can be improved by increasing the number of mirror pairs or optimizing the design of the structure [23–25], and a representative type of cavity structure is the DBR-cavity structure modified with the embedded submicrometer Gaussian-shaped defect. This structure is proposed by Ding *et al.*; relative to traditional DBR structures with the same number of mirror pairs, its quality factor can be effectively improved by nearly two orders of magnitude [25]. Physically, when the Gaussian-shaped defect is sandwiched between the upper and the lower Bragg mirrors, due to the local change in cavity length and the deformation of the photonic defect band, the photons are confined in a small modal volume in the vertical direction. Moreover, the light scattering induced by the lateral dielectric discontinuities is

*wangzy@sari.ac.cn

minimized. As a result, the quality of this structure dramatically improves. Based on the finite difference time domain (FDTD) calculation, the quality factors Q of the designed DBR cavity can exceed the order of 10^5 [25].

Here, we propose a hybrid planar DBR-cavity system, where IDTs are fabricated on the surface to generate the SAW. Moreover, the quality factor of the DBR cavity is optimized by the embedded Gaussian-shaped defect, and the DBR cavity is composed of AlAs and GaAs alternating layers, which are piezoelectric materials to support the SAW generation. When the SAW is applied to the system, we can estimate that the thickness of the upper Bragg mirrors is within the wavelength scope of the SAW. As a result, the upper Bragg mirrors in the vertical direction vibrate as a BAR, which can be considered a mechanical resonator. Accordingly, our system is turned into a standard three-level optomechanical cavity system [26,27], which is formed by the energy levels of the DBR cavity and BAR.

The traditional three-level optomechanical cavity system is composed of an optical cavity and a mechanical resonator; it has been applied in many fields, and a representative system is the optomechanically induced transparency (OMIT) [28–38]. OMIT is a special optical phenomenon. When it occurs, the susceptibility of the optomechanical cavity system changes; then, the resonance optical field can be modulated from opacity to transparency. Physically, it arises from the quantum interference among different energy-level pathways [39–42]. Similar to the electromagnetically induced transparency (EIT) observed in three-level atomic systems [43,44], OMIT has been applied in many fields including quantum information processing [30], fast and slow light [34], and quantum optical storage [45].

In our system, we show that when a strong pump optical field and a weak probe optical field are simultaneously applied to the hybrid optomechanical cavity system, in the presence of the SAW, a transmission window can be obtained in the weak output probe field. This phenomenon arises because under the driving of the SAW, the upper Bragg mirrors vibrate as a BAR; then, the DBR cavity becomes a Λ-type three-level optomechanical system. Under quantum interference among different energy-level pathways, OMIT occurs; as a result, the transmission window is observed in the weak output probe field. Conversely, without the actuation of the SAW, the transmission window disappears.

Compared to traditional micro-nano-optomechanical cavity systems, we propose an artificial DBR optomechanical cavity system that can be applied in optical quantum information processing, such as optical switches and information storage. Moreover, our system has many advantages:

(i) The parameter settings of our system are flexible; in particular, both frequencies of the optical cavity and nanomechanical resonator can be autonomously and accurately designed according to the application requirements.

(ii) Our system combines radio-frequency and optical signals to realize the electrically controlled quantum optical information processing.

(iii) The relevant manufacturing technology of the DBR microcavity our system adopted is mature and feasible, and our system can be combined with quantum dots and quantum traps to expand to the field of quantum device integration.
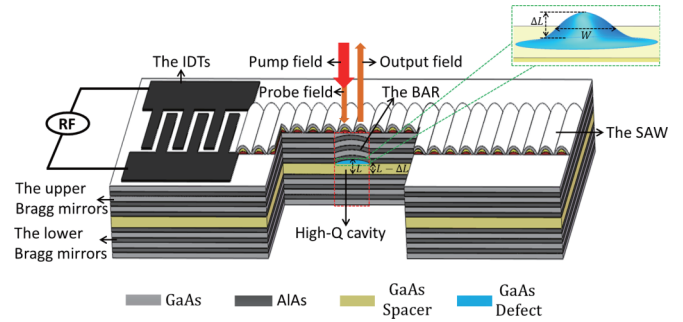

FIG. 1. Schematic diagram of the hybrid piezo-optomechanical DBR cavity system, where the IDTs are fabricated on the surface of the cavity to generate the SAW and the IDTs are driven by the RF voltage source. The high-Q planar DBR cavity (the area inside the red dashed box) is modified with the embedded Gaussian-shaped defect. The cavity is composed of AlAs (dark grey area) and GaAs (light grey area) alternating layers, and the GaAs spacer (dark yellow area) is sandwiched between the Bragg mirrors. L denotes the thickness of the DBR cavity, and $\triangle L$ and W denote the thickness and half width of the Gaussian-shaped defect (blue area), respectively. The optomechanical cavity is driven by a strong optical pump field (red arrow) and a weak optical probe field (brown arrow).

The paper is organized as follows. In Sec. II, we describe the proposed model and derive the system Hamiltonian. In Sec. III, we present the dynamical process of the system. In Sec. IV, we discuss the detailed physical mechanism of the OMIT and study the change in output field controlled by the SAW. Finally, we make a brief conclusion in Sec. V.

II. MODEL AND HAMILTONIAN OF THE SYSTEM

The hybrid piezo-optomechanical planar DBR-cavity system that we propose is illustrated in Fig. 1, where IDTs are fabricated on the surface of the cavity to generate the SAW. The IDTs are driven by the RF voltage source, which can convert the RF voltage signal to SAW via the piezoelectric effect. The high-Q cavity planar DBR cavity is modified with the embedded Gaussian-shaped defect, as designed by Ding *et al.* to improve the quality factor of the cavity [25]. The optomechanical cavity is driven by a strong optical pump field and a weak optical probe field. In detail, in our system, the quarter-wavelength design for the DBR mirrors is used to maximize the photon confinement. The DBR cavity is composed of AlAs and GaAs alternating layers. The GaAs spacer is sandwiched between the upper (10 pairs) and the lower (15 pairs) Bragg mirrors, and the same structure was applied in the recent experiment in Ref. [14].

Correspondingly, based on the design of the embedded Gaussian-shaped defect DBR-cavity structure, the photons on resonance are confined in a small modal volume on the order of $(\lambda/n)^3$ (λ is the spacer optical thickness, and n is the refractive index of the spacer material), and the light scattering induced by the lateral dielectric discontinuities is minimized. As a result, the quality factor is improved by nearly two orders of magnitude relative to the traditional DBR-cavity structure [25].

First, we consider the situation where only a pump optical field and a probe optical field are simultaneously applied to the

DBR cavity, and the frequencies of optical fields are referred to as ω_{pu} and ω_{pr}, respectively. Moreover, we assume that the phase difference between the probe and pump fields is zero, and the phase difference is locked. In this situation, the DBR cavity is a standard two-level energy system, whose Hamiltonian is given by

$$H_I = \omega_a \hat{a}^\dagger \hat{a} + i\hbar\varepsilon_{pu}(\hat{a}^\dagger e^{-i\omega_{pu}t} - \hat{a}e^{i\omega_{pu}t})$$
$$+ i\hbar\varepsilon_{pr}(\hat{a}^\dagger e^{-i\omega_{pr}t} - \hat{a}e^{i\omega_{pr}t}). \qquad (1)$$

Here, the first term of H_I describes the energy of the cavity mode, where ω_a is the frequency of the DBR cavity mode. $\hat{a}^\dagger$ and $\hat{a}$ are the creation and annihilation operators of the cavity mode, respectively. The second and third terms describe the energies of the input optical fields, and $\varepsilon_{pu} = \sqrt{P_{pu}\kappa_a/(\hbar\omega_{pu})}$ and $\varepsilon_{pr} = \sqrt{P_{pr}\kappa_a/(\hbar\omega_{pr})}$ are the amplitudes of the optical pump field and probe field, respectively. P_{pu} and P_{pr} are the input powers of the optical pump field and optical probe field, respectively. κ_a is the decay rate of the optical DBR cavity.

When the RF voltage source is also applied to the IDTs, the SAW is generated, and the upper Bragg mirrors vibrate as a BAR. Then, the Hamiltonian of the BAR can be written as

$$H_b = \frac{\hat{p}^2}{2m_b} + \frac{1}{2}m_b\omega_b{}^2\hat{q}^2, \qquad (2)$$

where $\hat{q}$ and $\hat{p}$ are the position and momentum operators of the BAR, m_b is the mass of the BAR, and ω_b is the frequency of the BAR, which is equal to the frequency of the RF voltage source. When the upper Bragg mirrors are vibrated as a BAR, the thickness of the DBR cavity L is changed accordingly.

In our system, the driving power of the RF transmitted by the IDTs is represented as P_{rf}. Referring to the relevant study in Ref. [4], we also assume that the SAW energy is uniformly distributed between the surface and one wavelength deep; then, the cross-section area through which the SAW travels is determined as $A = l_{IDTs}\lambda_s = l_{IDTs}\frac{v_{SAW}}{\omega_b}2\pi$, where l_{IDTs} is the length of the IDTs' fingers, and v_{SAW} is the velocity of the SAW. According to the relevant research [4], the vibration amplitude of the BAR is given as

$$q_0 = \sqrt{\frac{P_{rf}}{4\pi\, l_{IDTs}v_{SAW}^2\rho_b\omega_b}}, \qquad (3)$$

where ρ_b is the average density of the BAR. Based on a recent experiment [14], the amplitude of the BAR in our system can exceed 1 pm.

For the BAR whose vibration amplitude is q_0, referring to the relevant study in Ref. [4], the total energy of it is given as $E_b = 2m_b\omega_b{}^2q_0{}^2$. Taking the derivative of energy E_b with respect to position, we can obtain the amplitude of driving force induced by the RF voltage source, which is

$$F_{rf} = 4m_b\omega_b{}^2q_0. \qquad (4)$$

Since the frequency of the RF voltage source is also ω_b, according to the relevant research [4], the Hamiltonian of the
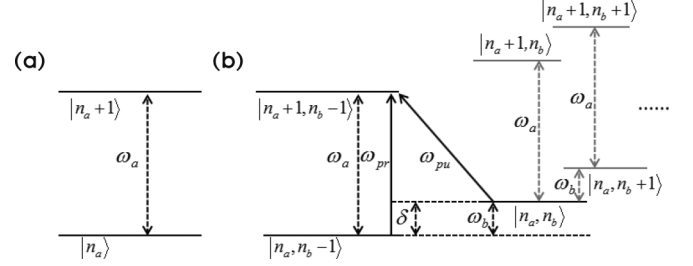

FIG. 2. (a) Energy-level structure of the hybrid optomechanical system (a) without and (b) with the SAW mode, where $|n_a\rangle$ and $|n_b\rangle$ are the number states of photons and phonons, respectively. The energy difference between $|n_a\rangle$ and $|n_a + 1\rangle$ is the frequency of the DBR cavity, ω_a, and the energy difference between $|n_b\rangle$ and $|n_b + 1\rangle$ is the frequency of the BAR, ω_b. Here, ω_{pr} is equal to ω_a, with the relation $\omega_{pr} - \omega_{pu} = \delta = \omega_b$.

system can be written as

$$H_O = \left(1 - \frac{\hat{q}}{L}\right)\omega_a\hat{a}^\dagger\hat{a} + i\hbar\varepsilon_{pu}(\hat{a}^\dagger e^{-i\omega_{pu}t} - \hat{a}e^{i\omega_{pu}t})$$
$$+ i\hbar\varepsilon_{pr}(\hat{a}^\dagger e^{-i\omega_{pr}t} - \hat{a}e^{i\omega_{pr}t}) + \frac{\hat{p}^2}{2m_b} + \frac{1}{2}m_b\omega_b{}^2\hat{q}^2$$
$$- F_{rf}q_0 sin(\omega_b t). \qquad (5)$$

Here, we assume that the phase difference between RF and optical fields is zero, and the phase difference is locked.

Now, we introduce the creation and annihilation operators for the BAR, which are

$$\hat{q} = \sqrt{\frac{\hbar}{2\omega_b m_b}}(\hat{b} + \hat{b}^\dagger), \quad \hat{p} = i\sqrt{\frac{\hbar\omega_b m_b}{2}}(\hat{b} - \hat{b}^\dagger), \qquad (6)$$

where $\hat{b}^\dagger$ and $\hat{b}$ are the creation and annihilation operators of the BAR, respectively. Then the Hamiltonian is rewritten as

$$H_O = \hbar\omega_a\hat{a}^\dagger\hat{a} + \hbar\omega_b\hat{b}^\dagger\hat{b} - \hbar g_{om}\hat{a}^\dagger\hat{a}(\hat{b} + \hat{b}^\dagger)$$
$$+ i\hbar\varepsilon_{pu}(\hat{a}^\dagger e^{-i\omega_{pu}t} - \hat{a}e^{i\omega_{pu}t}) + i\hbar\varepsilon_{pr}(\hat{a}^\dagger e^{-i\omega_{pr}t} - \hat{a}e^{i\omega_{pr}t})$$
$$- i\hbar\varepsilon_{rf}(\hat{b}^\dagger + \hat{b})(e^{-i\omega_{pr}t} - e^{i\omega_{pr}t}), \qquad (7)$$

where $g_{om} = \frac{w_a}{L}\sqrt{\frac{\hbar}{2\omega_b m_b}}$ is the single-photon coupling strength, and $\varepsilon_{rf} = F_{rf}\sqrt{\frac{1}{8\hbar\omega_b m_b}}$ is the amplitude of the RF voltage source. As a result, the initial two-level energy cavity system becomes a standard three-level energy optomechanical system, as shown in Fig. 2. In the frame that rotates at the frequency of the pump field, with respect to $H' = \hbar\omega_{pu}\hat{a}^\dagger\hat{a} - \hbar\omega_b\hat{b}^\dagger\hat{b}$ and neglecting the fast oscillating terms at the frequencies $\pm 2\omega_a$, $\pm 2\omega_b$, the Hamiltonian of the system is rewritten as

$$H_O = \hbar\Delta_a\hat{a}^\dagger\hat{a} + \hbar\omega_b\hat{b}^\dagger\hat{b} - \hbar g_{om}\hat{a}^\dagger\hat{a}(\hat{b}^\dagger + \hat{b})$$
$$+ i\hbar\varepsilon_{pu}(\hat{a}^\dagger - \hat{a}) + i\hbar\varepsilon_{pr}(\hat{a}^\dagger e^{-i\delta t} - \hat{a}e^{i\delta t}) + i\hbar\varepsilon_{rf}(\hat{b}^\dagger - \hat{b}),$$
$$(8)$$

where $\Delta_a = \omega_a - \omega_{pu}$ is the frequency detuning of the optical cavity from the pump field, and $\delta = \omega_{pr} - \omega_{pu}$ is the frequency detuning of the optical probe field from the pump field.

By combining the amplitude q_0 of the BAR with the creation and annihilation operators, the mean values of the creation and annihilation operators of the BAR are $\langle \hat{b} \rangle = \langle \hat{b}^\dagger \rangle = b_0$ [4], and we can obtain

$$q_0 = \sqrt{\frac{\hbar}{2\omega_b m_b}} 2b_0 = \sqrt{\frac{\hbar}{2\omega_b m_b}} 2\sqrt{n_0}, \qquad (9)$$

where $b_0 = q_0 \sqrt{\frac{\omega_b m_b}{2\hbar}}$ is the average amplitude of the BAR phonon operator, and n_0 is the initial mean phonon number of the BAR produced by the SAW. Moreover, we can obtain the relation of the average BAR phonon amplitude and RF voltage source amplitude, which is shown as $b_0 = \frac{\varepsilon_{rf}}{2\omega_b}$.

III. DYNAMICS OF THE SYSTEM

In our system, we consider the situation where the intensities of the optical pump field and the probe field satisfy the condition $\varepsilon_{pr} \ll \varepsilon_{pu}$. The system is operated in a resolved sideband regime, which satisfies the condition $\omega_b \sim \kappa_a$ [40]. Now, we adopt the quantum Langevin equations (QLEs) for the operators, where the damping and noise terms are supplemented [10,42]. Then, the Heisenberg-Langevin equations of the cavity mode and BAR mode can be obtained as

$$\dot{a} = -\left(i\Delta_a + \frac{\kappa_a}{2}\right)\hat{a} + ig_{om}\hat{a}(\hat{b}^\dagger + \hat{b}) + \varepsilon_{pu} + \varepsilon_{pr}e^{-i\delta t} + \hat{f},$$

$$\dot{b} = -\left(i\omega_b + \frac{\gamma_b}{2}\right)\hat{b} + ig_{om}\hat{a}^\dagger\hat{a} + \varepsilon_{rf} + \hat{\xi}. \qquad (10)$$

Here, $\hat{f}$ and $\hat{\xi}$ are the quantum and thermal noise operators, respectively [10]. γ_b is the intrinsic damping rate of the BAR.

Then, we linearize the dynamical equations of the operators by assuming $a = a_s + \delta a$, $b = b_s + \delta b$, which are both composed of an average amplitude and a fluctuation term. Here, a_s and b_s are the steady-state values of the operators when only the strong driving field is applied to the system. By assuming $\varepsilon_{pr} \to 0$ and setting all time derivatives to zero, we obtain

$$a_s = \frac{\varepsilon_{pu}}{i\Delta_a' + \frac{\kappa_a}{2}}, \quad b_s = \frac{ig_{om}|a_s|^2 + \varepsilon_{rf}}{i\omega_b + \frac{\gamma_b}{2}}, \qquad (11)$$

where $\Delta_a' = \Delta_a - g_{om}(b_s^* + b_s)$ denotes the effective frequency detuning of the optical pump field from the optical cavity, including the frequency shift caused by the mechanical motion. In our system, to ensure a strong-strength coupling between the optical pump field and the BAR, we consider the situation where the cavity is driven near the red sideband with $\Delta_a' \sim \omega_b$ [39].

Next, by substituting the assumptions $\hat{a} = a_s + \delta\hat{a}$ and $\hat{b} = b_s + \delta\hat{b}$ into the nonlinear QLEs and dropping the small nonlinear terms, we can obtain the linearized QLEs, which are

$$\dot{\delta\hat{a}} = -\left(i\Delta_a' + \frac{\kappa_a}{2}\right)\delta\hat{a} + iG_{om}(\delta b^\dagger + \delta\hat{b}) + \varepsilon_p e^{-i\delta t} + \hat{f},$$

$$\dot{\delta\hat{b}} = -\left(i\omega_b + \frac{\gamma_b}{2}\right)\delta\hat{b} + i(G_0^*\delta a + G_0\delta a^\dagger) + \hat{\xi}, \qquad (12)$$

where $G_{om} = g_{om}a_s$ is the total coupling strength between the optical mode and BAR mode.

Furthermore, the fluctuation terms can be rewritten as

$$\delta\hat{a} = \delta\hat{a}_+ e^{-i\delta t} + \delta\hat{a}_- e^{i\delta t}, \quad \delta\hat{b} = \delta\hat{b}_+ e^{-i\delta t} + \delta\hat{b}_- e^{i\delta t},$$

$$\delta\hat{f} = \delta\hat{f}_+ e^{-i\delta t} + \delta\hat{f}_- e^{i\delta t}, \quad \delta\hat{\xi} = \delta\hat{\xi}_+ e^{-i\delta t} + \delta\hat{\xi}_- e^{i\delta t}, \qquad (13)$$

where $\delta\hat{O}_+$ and $\delta\hat{O}_-$ (with $O = a, b$) correspond to the components at the original frequencies of ω_{pr} and $2\omega_{pu} - \omega_{pr}$, respectively [46,47]. Next we substitute Eqs. (13) into Eqs. (12) and ignore the second-order small terms by equating coefficients of terms with the same frequency, and the components at the frequencies ω_{pr} can be obtained as

$$\dot{\delta\hat{a}}_+ = \left(i\lambda_a - \frac{\kappa_a}{2}\right)\delta\hat{a}_+ + iG_{om}\delta\hat{b}_+ + \varepsilon_{pr} + \delta\hat{f}_+,$$

$$\dot{\delta\hat{b}}_+ = \left(i\lambda_b - \frac{\gamma_b}{2}\right)\delta\hat{b}_+ + iG_0^*\delta\hat{a}_+ + \delta\hat{\xi}_+, \qquad (14)$$

where $\lambda_a = \delta - \Delta_a'$, $\lambda_b = \delta - \omega_b$.

Next, we take the expectation values of the operators in our system. The noise terms obey the following fluctuations in correlation:

$$\langle \hat{f}_{in}(t)\hat{f}_{in}^\dagger(t') \rangle = [N(\omega_a) + 1]\delta(t - t'),$$

$$\langle \hat{f}_{in}^\dagger(t)\hat{f}_{in}(t') \rangle = [N(\omega_a)]\delta(t - t'),$$

$$\langle \hat{\xi}_{in}(t)\hat{\xi}_{in}^\dagger(t') \rangle = [N(\omega_c) + 1]\delta(t - t'),$$

$$\langle \hat{\xi}_{in}^\dagger(t)\hat{\xi}_{in}(t') \rangle = [N(\omega_c)]\delta(t - t'), \qquad (15)$$

where $N(\omega_a) = [\exp(\hbar\omega_a/k_B T) - 1]^{-1}$ is the equilibrium mean thermal photon numbers of the optical fields and $N(\omega_b) = [\exp(\hbar\omega_b/k_B T) - 1]^{-1}$ is the equilibrium mean thermal phonon number of the BAR.

We can safely assume that the optical field satisfies the condition $\hbar\omega_a/k_B T \gg 1$ at room temperature. For the BAR driven by the SAW, whose frequency is in the gigahertz regime, the environment temperature in the millidegrees Kelvin regime, which can be reached inside a dilution refrigerator, is sufficient to ensure that $\hbar\omega_b/k_B T \gg 1$ [26,48]. We assume that our system is operated in the millidegrees Kelvin temperature regime, and the quantum and thermal noise terms can be ignored.

Under the mean-field steady-state condition $\langle \dot{\delta\hat{a}} \rangle = \langle \dot{\delta\hat{b}} \rangle = 0$, we can get the solution of $\langle \delta\hat{a}_+ \rangle$, which is

$$\langle \delta\hat{a}_+ \rangle = \frac{\left(\frac{\gamma_b}{2} - i\lambda_b\right)\varepsilon_{pr}}{\left(\frac{\kappa_a}{2} - i\lambda_a\right)\left(\frac{\gamma_b}{2} - i\lambda_b\right) + G_{om}^2}. \qquad (16)$$

Based on the input-output relation, the output field at the probe frequency ω_{pr} can be expressed as [39,47]

$$\varepsilon_{out} = \kappa_a\langle \delta\hat{a}_+ \rangle - \varepsilon_{pr}. \qquad (17)$$

Then the transmission coefficient t_{pr} of the probe field is given by [27,42]

$$t_{pr} = \frac{\varepsilon_{out}}{\varepsilon_{pr}} = \frac{\kappa_a\langle \delta\hat{a}_+ \rangle}{\varepsilon_{pr}} - 1. \qquad (18)$$

By defining $\varepsilon_T = \frac{\kappa_a\langle \delta\hat{a}_+ \rangle}{\varepsilon_{pr}}$, we can obtain the quadrature ε_T of the output field at frequency ω_{pr}, which is

$$\varepsilon_T = \frac{\kappa_a\left(\frac{\gamma_b}{2} - i\lambda_b\right)}{\left(\frac{\kappa_a}{2} - i\lambda_a\right)\left(\frac{\gamma_b}{2} - i\lambda_b\right) + G_{om}^2}, \qquad (19)$$

which has the standard form for the OMIT [39]. The real part $\text{Re}[\varepsilon_T]$ and imaginary part $\text{Im}[\varepsilon_T]$ describe the absorptive and dispersive behaviors of the system, respectively. Correspondingly, the power transmission coefficient is further defined as

$$T_{pr} = |\, t_{pr}\,|^2. \qquad (20)$$

Moreover, the phase ϕ_T of the output field can be given as [49]

$$\phi_T = \arg[\varepsilon_T] = \frac{1}{2i}\text{Im}\left(\frac{\varepsilon_T}{\varepsilon_T^*}\right). \qquad (21)$$

In the red sideband region, the rapid phase dispersion can cause the group delay τ_T of the probe field, which can be expressed as

$$\tau_T = \frac{\partial \phi_T}{\partial \omega_{pr}} = \text{Im}\left[\frac{1}{\varepsilon_T}\frac{\partial \varepsilon_T}{\partial \omega_{pr}}\right]. \qquad (22)$$

IV. SAW-CONTROLLED OMIT AND PHYSICAL MECHANISM OF THE SYSTEM

We present below a discussion of the feasibility of the tunable OMIT in the hybrid piezo-optomechanical cavity system. In our system, the parameters that we used are described above, all of which are based on realistic systems. For the high-Q DBR cavity, the thicknesses of the GaAs and AlAs layers are $\lambda/4n_{\text{GaAs}} \sim 64.8$ nm (refractive index $n_{\text{GaAs}} = 3.57$) and $\lambda/4n_{\text{AlAs}} \sim 77.6$ nm (refractive index $n_{\text{AlAs}} = 2.98$), respectively. Correspondingly, the GaAs spacer optical thickness of the DBR cavity is $\lambda = 925$ nm, the corresponding frequency is $\omega_a = 324$ THz, and the actual thickness is $L = \lambda/n_{\text{GaAs}} = 259.1$ nm. To improve the quality of the DBR cavity, referring to the same structure proposed by Ding *et al.*, the shape of the defect is defined by the Gaussian function $G(x) = \triangle L e^{-x^2/2w^2}$, where $\triangle L$ and W are the thickness and half width, respectively, as shown in Fig. 1. In our system, we assume that $\triangle L = L/10 = 25.9$ nm and $W = L = 259.1$ nm. We can estimate that the quality factor of our system is increased to 10^5, and the corresponding cavity linewidth is approximately 3.5 GHz, so our system satisfies the condition of the sideband-resolved regime $\omega_b \sim \kappa_a$ [40].

The BAR is driven by the SAW, which is generated by the IDTs, and the length of the IDTs' fingers is $l_{\text{IDTs}} = 400\ \mu$m. The thickness of the upper ten pairs of Bragg mirrors is approximately 1.42 μm; as a result, it is within the wavelength scope of the SAW, whose wavelength is $\lambda_s = 2.9\ \mu$m. In our system, the selected frequency of the BAR is $\omega_b/2\pi = 1.05$ GHz, which was used in the recent experiment. Based on the related studies, the quality factor of the BAR exhibits the order of 10^5. Accordingly, we can estimate that the intrinsic damping rate of the BAR is $\gamma_b/2\pi = 10.5$ kHz, which satisfies the OMIT occurring condition $\kappa_a \gg \gamma_b$ [39]. Moreover, their material densities are $\rho_{\text{GaAs}} = 5.37$ g/cm^3 and $\rho_{\text{AlAs}} = 3.72$ g/cm^3, and we can estimate that the average density $\rho_b \sim 4.47$ g/cm^3 and the effective motional mass of the BAR is $m_b = 0.33$ pg. Then, based on the parameters that we use, the single-photon coupling strength can be estimated as $g_{om}/2\pi = 1.54 \times 10^7$ Hz.

Furthermore, to ensure that OMIT can be generated, the total optomechanical coupling strength should satisfy the con-
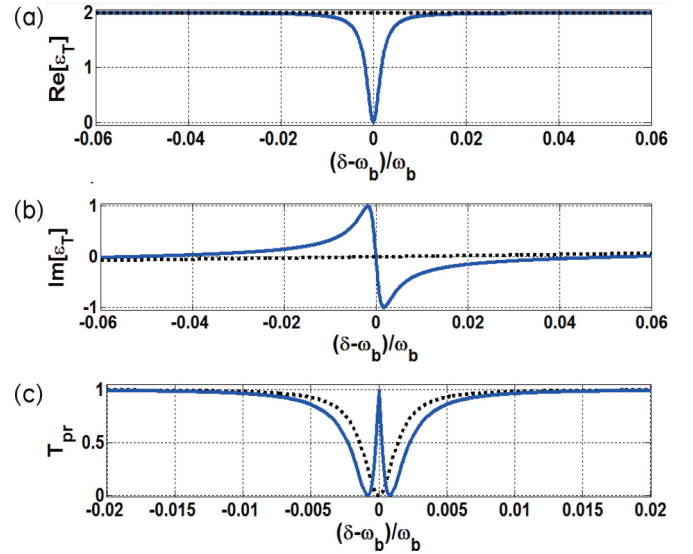

FIG. 3. (a) Real part $\text{Re}[\varepsilon_T]$, (b) imaginary part $\text{Im}[\varepsilon_T]$, and (c) power transmission coefficient T_{pr} of the optical probe field as functions of $(\delta - \omega_b)/\omega_b$. The solid blue line and dotted black line represent the situations with and without the SAW mode, respectively. The other parameters that we used are $\omega_a/2\pi = 324$ THz, $\kappa_a/2\pi = 3.5$ GHz, $\omega_b/2\pi = 1.05$ GHz, $\gamma_b/2\pi = 10.5$ kHz, $g_{om}/2\pi = 1.54 \times 10^7$ Hz, $P_{pu} = 0.015\ \mu$W, and $P_{rf} = 0.005$ W.

dition $G_{om} \geqslant \sqrt{\kappa_a\gamma_b}/2$, where a typical transmission window can be obtained [42]. Combining this condition with Eqs. (3) and (11) and dropping the small terms, we obtain the maximum power of the RF voltage source, which satisfies the relationship

$$P_{rf} \leqslant \left(\frac{8\hbar\pi\, l_{\text{IDTs}} v_{\text{SAW}}^2 \rho_b}{m_b}\right)\left(\varepsilon_{pu}\sqrt{\frac{1}{\kappa_a\gamma_b}} + \frac{\Delta_a}{2g_{om}}\right)^2, \quad (23)$$

where the relevant parameters are discussed and provided above. To ensure $b_0 \geqslant 1$, by combining Eqs. (3) and (9), we obtain the minimum power of the RF voltage source, which satisfies the relationship

$$P_{rf} \geqslant \frac{8\hbar\pi\, l_{\text{IDTs}} v_{\text{SAW}}^2 \rho_b}{m_b}. \qquad (24)$$

Next, we discuss the tunable OMIT behaviors of our system. First, based on the selected parameters, $\text{Re}[\varepsilon_T]$, $\text{Im}[\varepsilon_T]$ and the power transmission coefficient of the optical probe field as a function of $(\delta - \omega_b)/\omega_b$ are plotted in Fig. 3, and the solid blue line and dotted black line represent the situations with and without the SAW mode, respectively. When the SAW mode is absent, no transparency window can be obtained in the transmission spectrum curve. However, when the SAW mode is present, a transparency window is obtained in the transmission spectrum curve, whose center position is determined by the frequency point $\delta - \omega_b = 0$. As a result, our system can be applied in the fields of optical switches, high-resolution spectroscopy, and quantum information processing, which have been extensively studied [36,38].

The phenomenon in Fig. 3 arises as follows: when the SAW is absent, the initial system is a two-level cavity system, as shown in Fig. 2(a). It also corresponds to the situation where
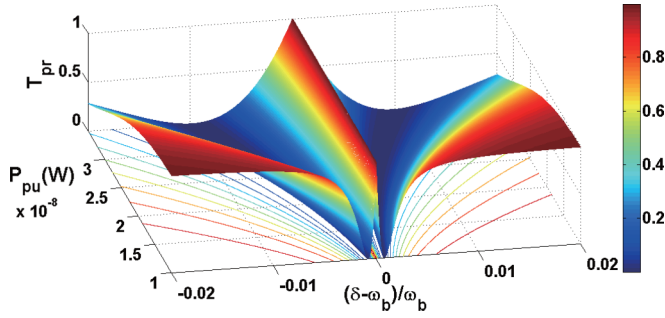
FIG. 4. Power transmission coefficient T_{pr} of the optical probe field as functions of $(\delta - \omega_b)/\omega_b$ and pump field power strength P_{pu}. P_{pu} is 1×10^{-8} to 3×10^{-8} W, and the other parameters are identical to those in Fig. 3.

FIG. 6. (a) Phase ϕ_T of the optical probe field as a function of $(\delta - \omega_b)/\omega_b$. (b) Group delay τ_T as a function of pump field power strength P_{pu}. The other parameters are identical to those in Fig. 3.

$g_{om} = 0$, referring to Eq. (1). As a result, the quantum interference between the energy levels cannot induce the occurrence of OMIT, and no transparency window appears. However, when the system is driven by the SAW, the upper Bragg mirrors vibrate as a BAR. Then, the initial two-level cavity system becomes a standard three-level optomechanical system, which is formed by the energy levels of the DBR cavity and BAR, as shown in Fig. 2(b). Under the effect of the optical radiation pressure, the destructive quantum interference between different energy-level pathways can be generated. Then, the OMIT phenomenon occurs, and a transparency window is obtained in the transmission spectrum curve. The relevant mechanism has been extensively studied [36,38,39].

Figure 4 presents the power transmission coefficient T_{pr} with respect to $(\delta - \omega_b)/\omega_b$ for different strengths P_{pu} of the optical pump field. In the presence of the SAW, when P_{pu} increases, the transmission window at the frequency position $\delta = \omega_b$ widens. The reason is that in the OMIT situation, the width Γ of the transmission window is proportional to the optical pump field power with the relations $\Gamma = \gamma_b + 4G_{om}^2/\kappa_a$ and $G_{om} = g_{om}a_s$, and the relevant mechanisms have been extensively studied [26]. As a result, this phenomenon can be applied in the fields of optical switches and optical quantum information process.

Figure 5 presents the power transmission coefficient T_{pr} with respect to $(\delta - \omega_b)/\omega_b$ for different powers P_{rf} of the

RF voltage source. When the SAW is generated by the IDTs, which is driven by the RF voltage source, with the increase in P_{rf}, the power transmission coefficient at frequency position $\delta = \omega_b$ decreases. The reason is that in the OMIT situation, the power transmission coefficient T_{pr} is proportional to the total coupling strength $G_{om} = g_{om}a_s$. Based on Eqs. (3), (9), and (11), the average phonon number a_s of the pump field can be determined by P_{rf}. With the increase in P_{rf}, the total coupling strength is diminished; hence, the power transmission coefficient at frequency position $\delta = \omega_b$ decreases. The minimum and maximum values of the RF voltage source power approximately correspond to transmission coefficients of 1 and 0, respectively, as presented in Eqs. (23) and (24). The relevant mechanisms have also been extensively studied [26]. This phenomenon can also be applied in the field of optical quantum information processing.

To further explore the characteristics of our system, when OMIT occurs, the phase ϕ_T as functions of $(\delta - \omega_b)/\omega_b$ and group delay τ_T as functions of pump field power strength P_{pu} are plotted in Fig. 6. Figure 6(a) shows that when OMIT occurs, the phase at frequency position $\delta = \omega_b$ is excessively modulated, which indicates that the group velocity of the probe field is altered. This situation generates a slow-light effect. Figure 6(b) shows that with increasing pump field power, the group delay of the probe field decreases. When the power of the pump field is sufficiently weak, the maximal time of the group delay can reach 0.03 ms. As a result, our system can be applied in the field of optical quantum information memory in solid-state systems.

V. CONCLUSION

In conclusion, we propose a scheme to generate tunable OMIT in a hybrid piezo-optomechanical cavity system. The system is composed of a high-quality planar DBR cavity modified with an embedded Gaussian-shaped defect. Moreover, IDTs are fabricated on the surface of the cavity and can generate the SAW under RF driving. We show that when a strong pump optical field and a weak probe optical field are applied to the hybrid optomechanical cavity system, in the presence of the SAW, a transmission window can be obtained
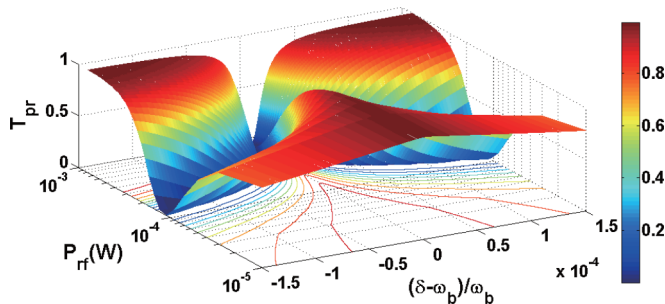

FIG. 5. Power transmission coefficient T_{pr} of the optical probe field as functions of $(\delta - \omega_b)/\omega_b$ and RF voltage source power P_{rf}. P_{rf} is 10^{-5} to 10^{-3} W, and the other parameters are identical to those in Fig. 3.
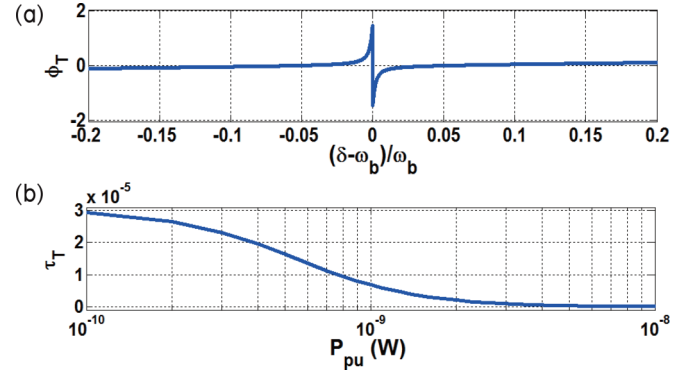
in the weak output probe field. In the presence of the SAW, the upper Bragg mirrors vibrate as a BAR, and the DBR cavity becomes a Λ-type three-level optomechanical system. As a result, the destructive quantum interference between different energy-level pathways generates OMIT, which makes a transmission window appear in the weak output probe field. Conversely, without the SAW, the transmission window in the weak output probe field disappears. Our scheme can be applied in the fields of optical switches, quantum information memory, high-resolution spectroscopy, and quantum information processing in solid-state systems.

[1] Z.-L. Xiang, S. Ashhab, J. Q. You, and F. Nori, Rev. Mod. Phys. **85**, 623 (2013).

[2] A. N. Cleland and M. R. Geller, Phys. Rev. Lett. **93**, 070501 (2004).

[3] J. Teissier, A. Barfuss, P. Appel, E. Neu, and P. Maletinsky, Phys. Rev. Lett. **113**, 020503 (2014).

[4] D. A. Golter, T. Oo, M. Amezcua, K. A. Stewart, and H. Wang, Phys. Rev. Lett. **116**, 143602 (2016).

[5] A. Dousse, J. Suffczyński, A. Beveratos, O. Krebs, A. Lemaître, I. Sagnes, J. Bloch, P. Voisin, and P. Senellart, Nature (London) **466**, 217 (2010).

[6] J. Kabuss, A. Carmele, T. Brandes, and A. Knorr, Phys. Rev. Lett. **109**, 054301 (2012).

[7] C. M. Fabre, P. Cheiney, G. L. Gattobigio, F. Vermersch, S. Faure, R. Mathevet, T. Lahaye, and D. Guéry-Odelin, Phys. Rev. Lett. **107**, 230401 (2011).

[8] O. Gazzano, S. Michaelis de Vasconcellos, C. Arnold, A. Nowak, E. Galopin, I. Sagnes, L. Lanco, A. Lemaítre, and P. Senellart, Nat. Commun. **4**, 1425 (2013).

[9] R. W. Andrews, R. W. Peterson, T. P. Purdy, K. Cicak, R. W. Simmonds, C. A. Regal, and K. W. Lehnert, Nat. Phys. **10**, 321 (2014).

[10] S. Barzanjeh, D. Vitali, P. Tombesi, and G. J. Milburn, Phys. Rev. A **84**, 042342 (2011).

[11] A. Gaidarzhy, G. Zolfagharkhani, R. L. Badzey, and P. Mohanty, Phys. Rev. Lett. **94**, 030402 (2005).

[12] J. Bochmann, A. Vainsencher, D. D. Awschalom, and A. N. Cleland, Nat. Phys. **9**, 712 (2013).

[13] M. M. de Lima, R. Hey, P. V. Santos, and A. Cantarero, Phys. Rev. Lett. **94**, 126805 (2005).

[14] M. Metcalfe, S. M. Carr, A. Muller, G. S. Solomon, and J. Lawall, Phys. Rev. Lett. **105**, 037401 (2010).

[15] M. M. de Lima and P. V. Santos, Rep. Prog. Phys. **68**, 1639 (2005).

[16] K. C. Balram, M. I. Davanço, B. R. Ilic, J.-H. Kyhm, J. D. Song, and K. Srinivasan, Phys. Rev. Appl. **7**, 024008 (2017).

[17] J. B. Kinzel, D. Rudolph, M. Bichler, G. Abstreiter, J. J. Finley, G. Koblmüller, A. Wixforth, and H. J. Krenner, Nano Lett. **11**, 1512 (2011).

[18] T. Sogawa, P. V. Santos, S. K. Zhang, S. Eshlaghi, A. D. Wieck, and K. H. Ploog, Phys. Rev. B **63**, 121307(R) (2001).

[19] M. J. A. Schuetz, E. M. Kessler, G. Giedke, L. M. K. Vandersypen, M. D. Lukin, and J. I. Cirac, Phys. Rev. X **5**, 031031 (2015).

[20] E. B. Magnusson, B. H. Williams, R. Manenti, M.-S. Nam, A. Nersisyan, M. J. Peterer, A. Ardavan, and P. J. Leek, Appl. Phys. Lett. **106**, 063509 (2015).

[21] M. M. de Lima, R. Hey, and P. V. Santos, Appl. Phys. Lett. **83**, 2997 (2003).

[22] P. Lacharmoise, A. Fainstein, B. Jusserand, and V. Thierry-Mieg, Appl. Phys. Lett. **84**, 3274 (2004).

[23] D. Lu, J. Ahn, H. Huang, and D. G. Deppe, Appl. Phys. Lett. **85**, 2169 (2004).

[24] M. Sudzius, M. Langner, S. I. Hintschich, V. G. Lyssenko, H. Fröb, and K. Leo, Appl. Phys. Lett. **94**, 061102 (2009).

[25] F. Ding, T. Stöferle, L. Mai, A. Knoll, and R. F. Mahrt, Phys. Rev. B **87**, 161116(R) (2013).

[26] M. Aspelmeyer, T. J. Kippenberg, and F. Marquardt, Rev. Mod. Phys. **86**, 1391 (2014).

[27] S. Weis, R. Rivière, S. Deléglise, E. Gavartin, O. Arcizet, A. Schliesser, and T. J. Kippenberg, Science **330**, 1520 (2010).

[28] L. Fan, K. Y. Fong, M. Poot, and H. X. Tang, Nat. Commun. **6**, 5850 (2015).

[29] M. Bienert and P. Barberis-Blostein, Phys. Rev. A **91**, 023818 (2015).

[30] K. Stannigel, P. Rabl, A. S. Sorensen, M. D. Lukin, and P. Zoller, Phys. Rev. A **84**, 042341 (2011).

[31] X. W. Xu, Y. X. Liu, C. P. Sun, and Y. Li, Phys. Rev. A **92**, 013852 (2015).

[32] L. G. Si, H. Xiong, M. S. Zubairy, and Y. Wu, Phys. Rev. A **95**, 033803 (2017).

[33] J. Ma, C. You, L. G. Si, H. Xiong, J. Li, X. Yang, and Y. Wu, Sci. Rep. **5**, 11278 (2015).

[34] M. J. Akram, M. M. Khan, and F. Saif, Phys. Rev. A **92**, 023846 (2015).

[35] Q. Wang, J. Q. Zhang, P. C. Ma, C. M. Yao, and M. Feng, Phys. Rev. A **91**, 063827 (2015).

[36] H. Wang, X. Gu, Y.-x. Liu, A. Miranowicz, and F. Nori, Phys. Rev. A **90**, 023817 (2014).

[37] Z. Duan, B. Fan, T. M. Stace, G. J. Milburn, and C. A. Holmes, Phys. Rev. A **93**, 023802 (2016).

[38] P.-C. Ma, J.-Q. Zhang, Y. Xiao, M. Feng, and Z.-M. Zhang, Phys. Rev. A **90**, 043825 (2014).

[39] G. S. Agarwal and S. Huang, Phys. Rev. A **81**, 041803(R) (2010).

[40] K. C. Balram, M. I. Davanco, J. D. Song, and K. Srinivasan, Nat. Photonics **10**, 346 (2016).

[41] A. H. Safavi-Naeini, T. M. Alegre, J. Chan, M. Eichenfield, M. Winger, Q. Lin, J. T. Hill, D. E. Chang, and O. Painter, Nature (London) **472**, 69 (2011).

[42] W. Z. Jia, L. F. Wei, Y. Li, and Y.-x. Liu, Phys. Rev. A **91**, 043843 (2015).

[43] S. E. Harris, Phys. Today **50**(7), 36 (1997).

[44] K. J. Boller, A. Imamoglu, and S. E. Harris, Phys. Rev. Lett. **66**, 2593 (1991).

[45] S. A. McGee, D. Meiser, C. A. Regal, K. W. Lehnert, and M. J. Holland, Phys. Rev. A **87**, 053818 (2013).

[46] S. Huang and G. S. Agarwal, Phys. Rev. A **83**, 023823 (2011).

[47] J.-Q. Zhang, Y. Li, M. Feng, and Y. Xu, Phys. Rev. A **86**, 053806 (2012).

[48] A. Cleland, Nat. Phys. **5**, 458 (2009).

[49] K.-H. Gu, X.-B. Yan, Y. Zhang, C.-B. Fu, Y.-M. Liu, X. Wang, and J.-H. Wu, Opt. Commun. **338**, 569 (2015).